

# Interaction of a Streamwise Vortex with a Free Surface

Turgut Sarpkaya\* and Donald E. Neubert†  
Naval Postgraduate School, Monterey, California 93943

**An experimental investigation on the flow structure resulting from the interaction of a single tip vortex with a deformable free surface is described. The results have shown that the free surface redistributes part or all of the normal turbulent kinetic energy into streamwise and spanwise components. The turbulent kinetic energy first decreases sharply with increasing vertical distance from the vortex and then remains nearly constant within a thin layer below the "roughened" free surface. The results lend further credence to the simulation of near-surface structures by a decaying two-dimensional turbulence via vortex or contour dynamics.**

## Nomenclature

$AR$	= aspect ratio of foil
$b_0$	= semispan of foil
$c$	= chord length of foil
$h$	= $z$ position of a horizontal plane from vortex
$h_0$	= depth of vortex from free surface
$Re$	= Reynolds number, $U_0 c / \nu$
$t$	= time
$U_0$	= velocity of ambient flow
$u$	= axial component of velocity
$u'$	= rms value of $u'$ , normalized by $U_0$
$V_0$	= maximum velocity in vortex
$v$	= transverse component of velocity
$v'$	= rms value of $v'$ , normalized by $U_0$
$w$	= vertical component of velocity
$w'$	= rms value of $w'$ , normalized by $U_0$
$x$	= axial coordinate, origin at vortex
$x'$	= axial coordinate, origin at free surface
$y$	= lateral coordinate, origin at vortex
$y'$	= lateral coordinate, origin at free surface
$Z$	= complex variable, $y' + iz'$ , origin at free surface
$z$	= vertical coordinate, origin at vortex
$z'$	= vertical coordinate, origin at free surface
$\Gamma$	= circulation of vortex
$\zeta$	= $h / \sigma_0$
$\zeta_0$	= $h_0 / \sigma_0$
$\eta$	= $y / \sigma_0$
$\kappa$	= $\Gamma / 2\pi$
$\xi$	= $x / \sigma_0$
$\sigma_0$	= vortex core radius

## Introduction

THE unsteady flow phenomena resulting from the interaction of wakes and vortices with the free surface are of particular importance in naval hydrodynamics. Ship wakes produce a three-dimensional complex signature, comprised of a narrow dark band bordered by two bright lines in synthetic-aperture-radar (SAR) images. The dark band is the most prominent of all of the signatures and is seen many kilometers downstream at all angles to the SAR azimuth direction even under severe weather conditions. It signifies the suppression of waves at the Bragg frequency as a consequence of various

short-wave-damping phenomena such as turbulence, surface-active materials, and the redistribution of surface impurities. The two bright lines, on the other hand, each resembling a moon glade, manifest themselves only in light winds and signify the occurrence of a range of waves that happen to be near the Bragg wavelength, possibly as a consequence of the interaction between quasi-two-dimensional turbulent motions near the free surface and the restructuring and modulation of this interaction by wind.

The foregoing strongly suggests that the three-dimensional turbulent flowfield beneath the free surface, the extent of the two-dimensionalization of turbulence with depth, and the reverse energy cascade process near the free surface must be understood in as much detail as possible to gain some insight into the occurrence of surface signatures. One of the simplest possible flows relevant to the dynamical processes in vorticity/free-surface interaction that can be carefully studied in isolation, without complications and competing influences that normally occur in a fully turbulent ship wake, is the interaction of a single turbulent vortex with the free surface of an otherwise smooth uniform flow. The modulations of the flowfield and turbulence near the free surface are not expected to be similar to that observed for a streamwise vortex in or near a rigid-wall boundary layer.<sup>1,2</sup>

Extensive reviews of the interaction of a pair of heterostrophic vortices with a free surface are given by Sarpkaya,<sup>3-5</sup> Sarpkaya et al.,<sup>6</sup> and Sarpkaya and Suthon<sup>7</sup> wherein it is suggested that the free-surface signatures (scars) exhibit features that obey the decay laws of two-dimensional turbulence. The reverse energy cascade process dominates the turbulence behavior near the free surface through the interaction and merging of homostrophic vortices. The energy and enstrophy inertial ranges coexist, with an upscale energy transfer and downscale enstrophy transfer in the same wave number interval. The quasi-two-dimensionalization of turbulence in various types of flows,<sup>8-9</sup> in general, and near a free surface,<sup>10-18</sup> in particular, has emerged as a fundamental phenomenon during the past decade.

## Experimental Equipment

The experiments were conducted in a low-turbulence water tunnel with an open test section 40 cm wide, 50 cm deep (maximum), and 150 cm long. The turbulence management system was located upstream of the test section. It consisted of a honeycomb and a fine-mesh screen. The tunnel was driven by a 50-hp centrifugal pump. A second but smaller pump continuously circulated the tunnel water through a microfiltration system to remove rust and other suspended fine particles, down to about 1  $\mu\text{m}$ , from the water (the filtration system was turned off during the experiments). A skimmer, placed upstream of the turbulence management system and connected to another filter, was operated continuously to maintain the free surface clean.

Received Jan. 9, 1993; presented as Paper 93-0556 at the AIAA 31st Aerospace Sciences Meeting, Reno, NV, Jan. 11-14, 1993; revision received July 2, 1993; accepted for publication July 7, 1993. This paper is declared a work of the U.S. Government and is not subject to copyright protection in the United States.

\*Distinguished Professor of Mechanical Engineering. Associate Fellow AIAA.

†Lieutenant, United States Navy, Mechanical Engineering.

A 6% thick, rectangular planform, symmetric, Joukowski half-span foil with an effective aspect ratio of 10.4 was used to generate a "single" trailing vortex. The tip of the foil was carefully rounded. The model foil was mounted in a rotatable cylindrical base, embedded into the bottom of the test section floor. The angle of attack was set at 12 deg and the water level was held constant. The interior of the model was hollowed and connected to a dye reservoir to seed the vortex core with a fluorescent dye. The leading edge of the foil was 3.6 chord lengths downstream of the test section entrance. The lateral position of the foil was offset by about two vortex-core radii so that the vortex entered the working section fairly near the midplane where the measurements are made. The reason for the offset is that there is necessarily a wake side wash (a flux of lateral momentum) due to the lift or the transverse force of magnitude  $\rho U_0 \Gamma b_0$  acting on the foil.

The total circulation of the fully submerged vortex was calculated from the tangential velocity distribution and from (Durand<sup>19</sup>)

$$\Gamma/U_0 c = [1.05\pi(\alpha - \alpha_0)]/(1 + 2/AR) \quad (1)$$

including a correction for the wall effect of the tunnel floor. The calculated values were within 1% of that obtained from the tangential velocity distribution.

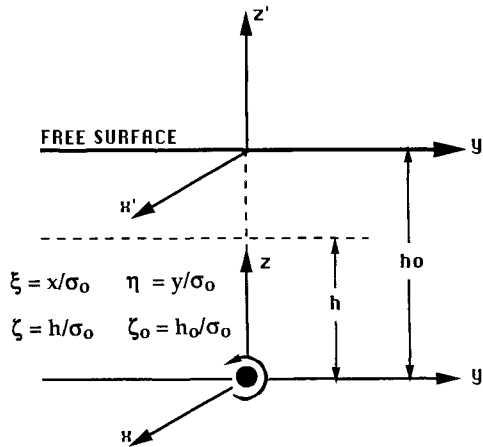


Fig. 1 Coordinate definition.

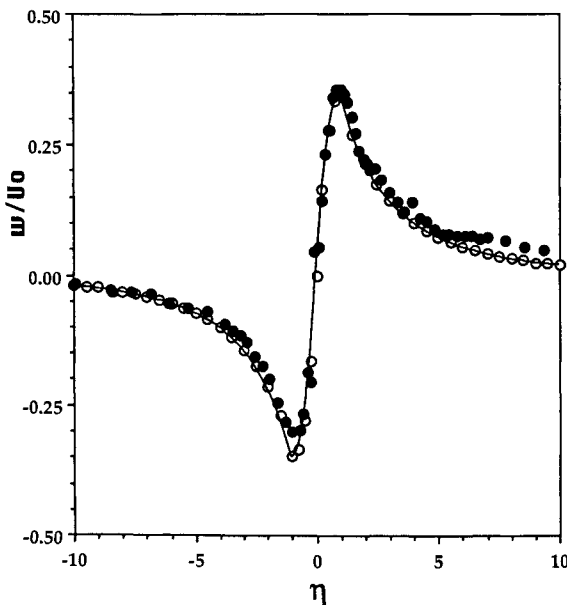


Fig. 2 Horizontal profile of  $w/U_0$  at  $\zeta = 0$  for  $\zeta_0 = 3.85$  (full symbols: data, open symbols: analysis).

The mean velocities and turbulence intensities were measured with a laser-doppler anemometer. Bragg-cell frequency shifting by 40 MHz was used in both channels to detect the flow reversals. The probe volume (approximately 200  $\mu\text{m}$  in diameter) was positioned at the required location by use of a remotely driven  $x$ - $y$ - $z$  traversing unit. The scattering particles used were titanium dioxide of rutile crystalline form and were approximately 3  $\mu\text{m}$  in size. All measurements were made using 1024 point ensembles. The data are reported without any velocity bias correction.

The initial measurements were dedicated to the establishment of the flow characteristics at the test section. These measurements have shown that the velocity was uniform (except in the boundary layers, of course) within 0.5%, in both the vertical and horizontal directions. The freestream turbulence level was about 0.3%. The extensive video recording of the vortex structure through the use of the laser-induced fluorescence (LIF) technique at various speeds ranging from 60 to 1000 frames/s has shown that there was very little or no "vortex wandering."

Two vortex positions relative to the free surface and two measurement stations relative to the trailing edge of the foil were considered. For the first case, named deeper submergence (DS), the vortex axis was placed at  $\zeta_0 = h_0/\sigma_0 = 8.3$  from the free surface. For the second case, named shallower submergence (SS), the vortex axis was placed at  $\zeta_0 = 3.85$  from the free surface. In both cases, the velocity and turbulence measurements were made along several  $\eta = \text{const}$  (vertical lines) and  $\zeta = \text{const}$  (horizontal lines) at three stations along the vortex (3.6, 5.6, and 13.6 chord lengths downstream from the trailing edge of the foil). Of the measurements made to date, only the data taken at 3.6 chord lengths downstream of the trailing edge, for a chord-based Reynolds number of  $U_0 c/\nu = 45 \times 10^4$ ,  $\Gamma/\nu = 2500$ , and a vortex circulation of  $\Gamma/U_0 c = 0.57$ , will be described in detail here, even though extensive data were taken at other values of the parameters cited earlier.

## Results and Discussion

A key to the quantification of the flowfield created by the interaction of the mean flow, longitudinal vortex, and the free surface was to establish a model for the vortex in terms of its core size  $\sigma_0$  and strength  $\Gamma$ . The Rankine and Lamb vortices were rejected as being unrepresentative of a trailing vortex. Instead, a Rosenhead<sup>20</sup> vortex was chosen. Then the vortex and its image above the free surface yield (see Fig. 1)

$$v - iw = -\frac{i\kappa}{(Z + ih_0)[(Z + ih_0)^2 + \sigma_0^2]} + \frac{i\kappa}{(Z - ih_0)[(Z - ih_0)^2 + \sigma_0^2]} \quad (2)$$

in which  $Z = y' + iz'$ , the complex variable;  $y'$  is the transverse coordinate; and  $z'$  is the surface-normal direction, with the origin at the free surface. The vortex strength is  $\kappa = \Gamma/2\pi$ , and  $-ih_0$  is the vertical position of the vortex in the  $y'$ - $z'$  plane. The transverse and vertical components of velocity ( $v$  and  $w$ ) along a horizontal line  $Z = y' - i(h_0 - h)$ , i.e.,  $z' = -(h_0 - h)$  or  $z = h$  (see Fig. 1) are given by

$$\frac{v}{V_0} = 1.548 \left[ \frac{\zeta}{\eta^2 + \zeta^2 + 1} + \frac{2\zeta_0 - \zeta}{\eta^2 + (2\zeta_0 - \zeta)^2 + 1} \right] \quad (3a)$$

and

$$\frac{w}{V_0} = \frac{2\eta}{(\eta^2 + \zeta^2 + 1)} - \frac{2\eta}{[\eta^2 + (2\zeta_0 - \zeta)^2 + 1]} \quad (3b)$$

in which  $\eta = y'/\sigma_0$ ,  $\zeta = h/\sigma_0$ ,  $\zeta_0 = h_0/\sigma_0$ , and  $V_0$  is the maximum tangential velocity at the edge of the vortex core. The free surface is given by  $\zeta = \zeta_0$  or by  $h = h_0$ .

The horizontal profiles of the  $w$  component of velocity at  $\zeta = 0$  are shown in Figs. 2 and 3 for the cases SS ( $\zeta_0 = 3.85$ )

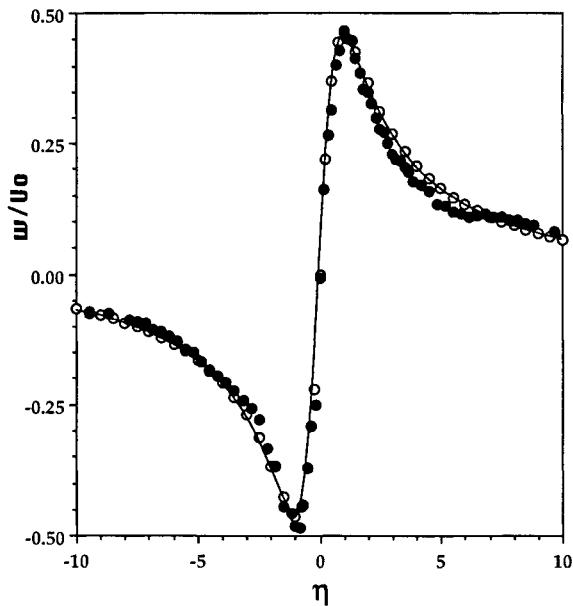


Fig. 3 Horizontal profile of  $w/U_0$  at  $\zeta = 0$  for  $\zeta_0 = 8.30$  (full symbols: data, open symbols: analysis).

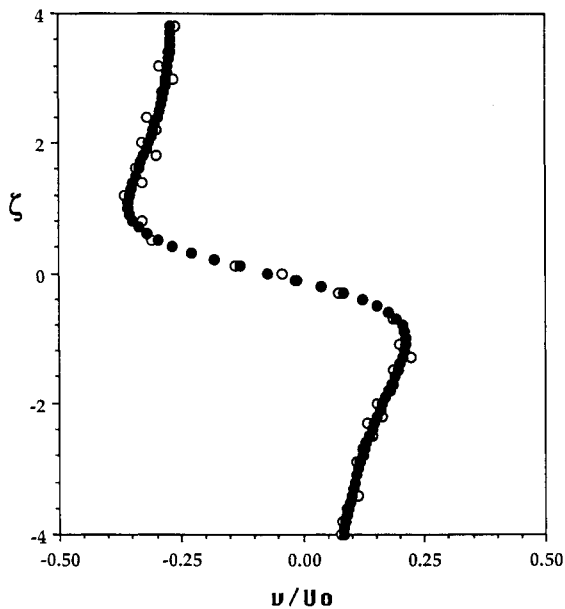


Fig. 4 Vertical profile of  $v/U_0$  for  $\eta = 0$  and  $\zeta_0 = 3.85$  (full symbols: data, open symbols: analysis).

and DS ( $\zeta_0 = 8.3$ ), respectively, in terms of  $w/U_0$ . The vertical profile of the  $y$  component of velocity at  $\eta = 0$  is shown in Fig. 4 in terms of  $v/U_0$  for  $\zeta_0 = 3.85$ . Strictly speaking, neither the shape of the vortex core nor the vortex strength can be precisely simulated with a relatively simple model because of the effect of the image flow (mutual straining of the vortex cores) and the free-surface deformation. Nevertheless, the measurements may be made to match those predicted from Eqs. (3a) and (3b) in terms of two experimentally determined values: core radius  $\sigma_0$  and the circulation  $\kappa$ . This is particularly true for the case DS, i.e., for a vortex that is sufficiently far from the free surface so as not to be materially affected by its image and the surface disturbances. Figure 2 shows the onset of the free-surface effects with a slight elevation of  $w/U_0$  in the region  $5 < \eta < 10$ .

The data in all velocity profiles exhibited very little scatter (two sets of data taken at different days are shown in the foregoing figures). Had there been vortex wandering, the

time-averaged Eulerian point measurements (then representing the weighted temporal and spatial averages of the velocity) would have shown large scatter, particularly in the regions of strong velocity gradients. As noted earlier, the video recordings of the vortex structures (in both the axial and transverse planes) have confirmed that there was no noticeable vortex wandering, at least at the measurement station.

The horizontal profile of the axial velocity defect is shown in Fig. 5 for  $\zeta = 0$  and  $\zeta_0 = 3.85$ . The region of strong velocity defect is confined to about two core radii. Within a distance of about  $3\sigma_0$ , the velocity defect drops to about 0.1 in both the horizontal and vertical profiles. Figure 6, for  $\zeta_0 = 3.85$  and  $\zeta = -2.31$  (i.e., in a plane below the foil tip), is particularly interesting because it exhibits simultaneously the effect of the nearly symmetrical small velocity defect (at least for  $\eta < 4$ ) and the effect of the foil wake (near  $\eta = 7$ , because of the wake side wash), resulting from the unrolled-up portion of the vorticity sheet. It is equally interesting to note that had there been no wake effect, the velocity defect profile could have smoothly joined between  $\eta = 4$  and 14. In fact, Fig. 5 shows

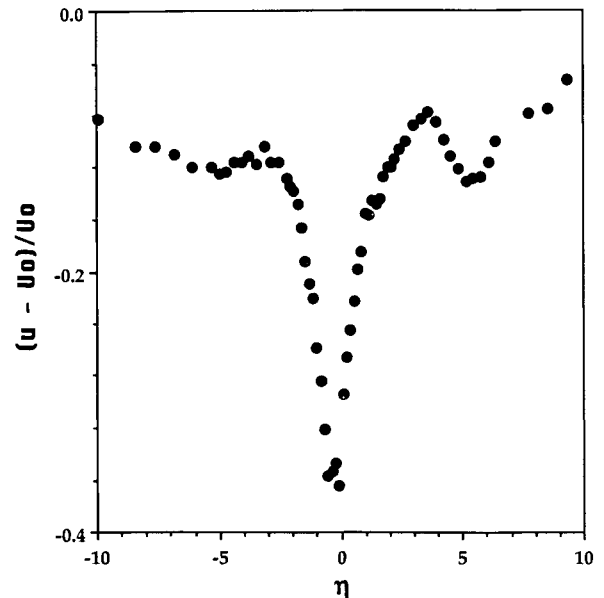


Fig. 5 Horizontal profile of the axial velocity defect at  $\zeta = 0$  for  $\zeta_0 = 3.85$ .

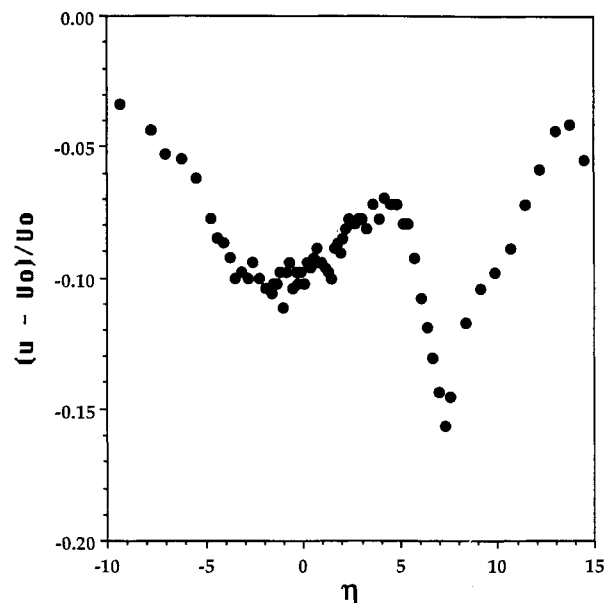


Fig. 6 Horizontal profile of the axial velocity defect at  $\zeta = 2.31$  for  $\zeta_0 = 3.85$ .

that for  $\zeta = 0$  the wake effect disappears and the velocity-defect profile becomes nearly symmetrical. For planes closer to the free surface, the results have shown that the velocity defect becomes very small and once again asymmetrical due to the deformation and proximity of the free surface.

The rms values of turbulence, normalized by  $U_0$  and denoted here by  $u'$ ,  $v'$ , and  $w'$ , will be discussed in terms of a relatively small number of figures, since the presentation of a large set of data, taken at various horizontal and vertical planes, is clearly impossible.

Figure 7 shows a representative horizontal profile of  $u'$  for  $\zeta = 0.77$  and  $\zeta_0 = 3.85$ . Two distinct regions are clearly identifiable. The  $u'$  directly above the vortex axis is rather large and falls to about 0.07 within a radius of  $\eta = 3$ . The second region, the side lobes of the first, is marked by a lower level  $u'$  and spans over a wider region, eventually reducing to about 0.05 within  $\eta < 10$ . Figure 8 shows the vertical profile of  $u'$  at  $\eta = 0$ , again for the case SS. Apparently,  $u'$  near the edge of the vortex core is slightly higher than that near the axis of the

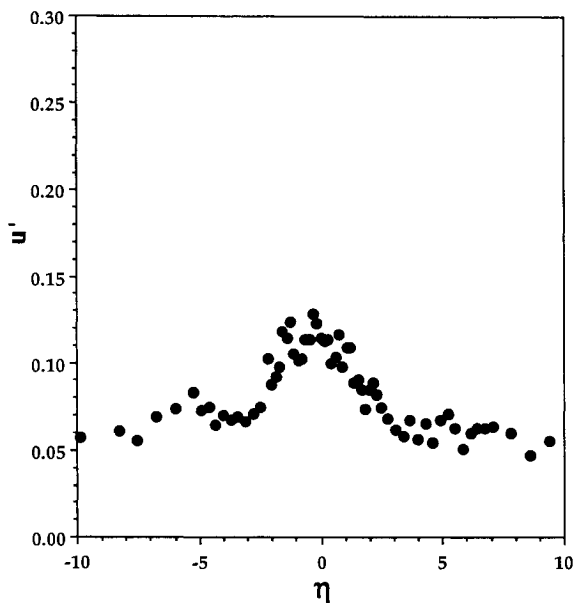


Fig. 7 Horizontal profile of the rms fluctuations in the axial direction at  $\zeta = 0.77$  for  $\zeta_0 = 3.85$ .

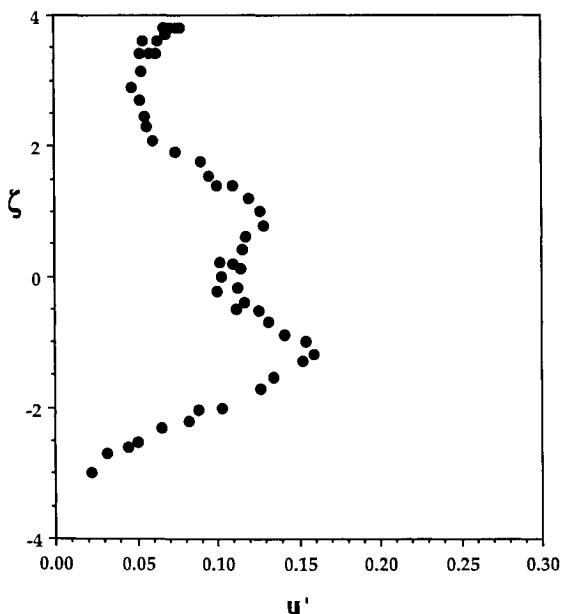


Fig. 8 Vertical profile of the rms fluctuations in the axial direction at  $\eta = 0$  for  $\zeta_0 = 3.85$ .

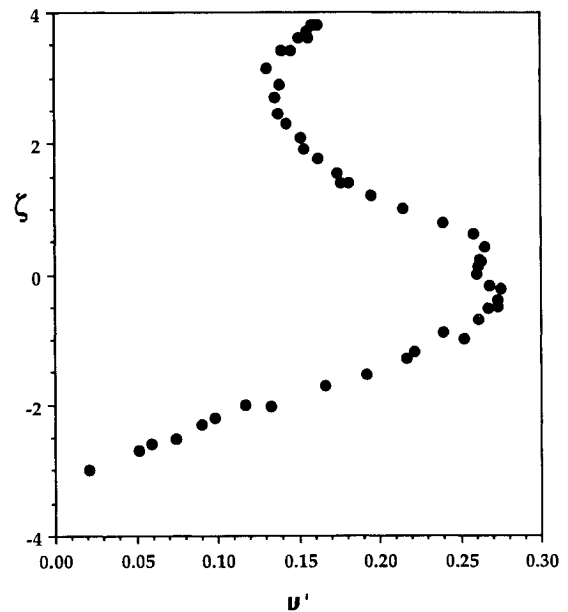


Fig. 9 Vertical profile of the rms fluctuations in the lateral direction at  $\eta = 0$  for  $\zeta_0 = 3.85$ .

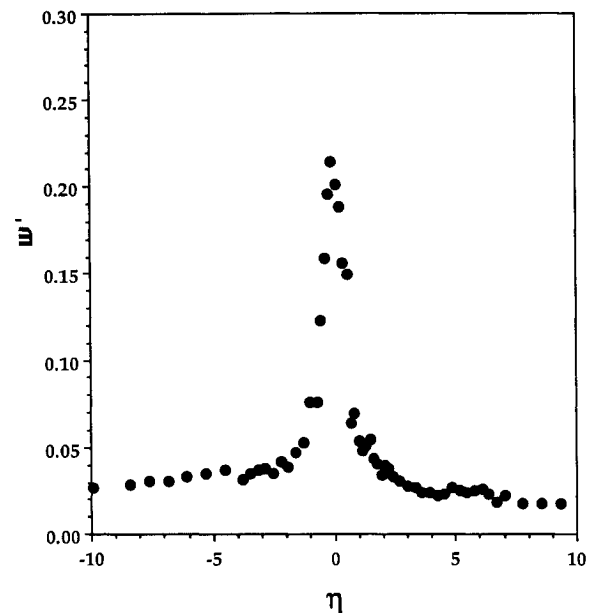


Fig. 10 Horizontal profile of the rms fluctuations in the vertical direction at  $\zeta = 0$  for  $\zeta_0 = 3.85$ .

vortex. Below the vortex axis,  $u'$  decreases rather rapidly, as would be expected. For positive values of  $\zeta$ , however,  $u'$  first decreases, as if it were symmetrical, and then increases very near the free surface, within a distance of about one core radius. This may not have been very interesting had it not been accompanied by other events. Figure 9 shows the vertical profile of  $v'$  in terms of  $\zeta$  for  $\eta = 0$  and  $\zeta_0 = 3.85$ . Once again, it is very large near the vortex axis but decreases sharply, and almost symmetrically, away from the core. Very near the free surface, however,  $v'$ , like  $u'$ , exhibits a relatively significant increase. On the basis of these observations, an increase in  $w'$  will require an explanation for the increase in turbulent kinetic energy, and a decrease in  $w'$  will signify the increase of anisotropy and the quasi-two-dimensionalization of an otherwise nearly isotropic turbulence.

Figures 10 and 11 show representative horizontal profiles of  $w'$  at  $\zeta = 0$  and at 0.77 for the case SS. Clearly,  $w'$  decreases

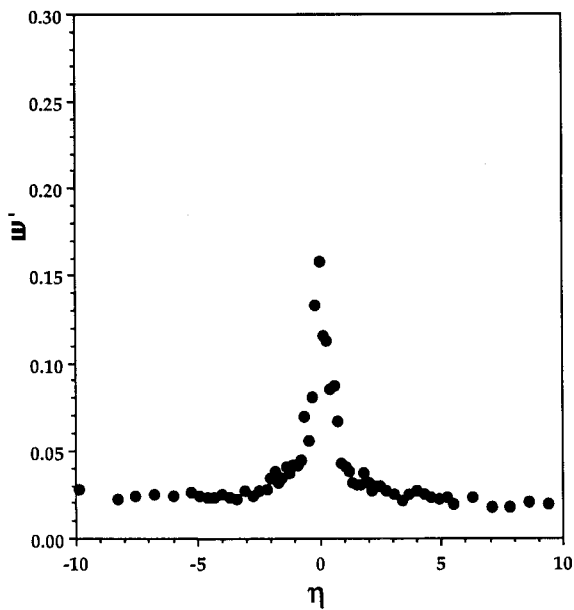


Fig. 11 Horizontal profile of the rms fluctuations in the vertical direction at  $\zeta = 0.77$  for  $\zeta_0 = 3.85$ .

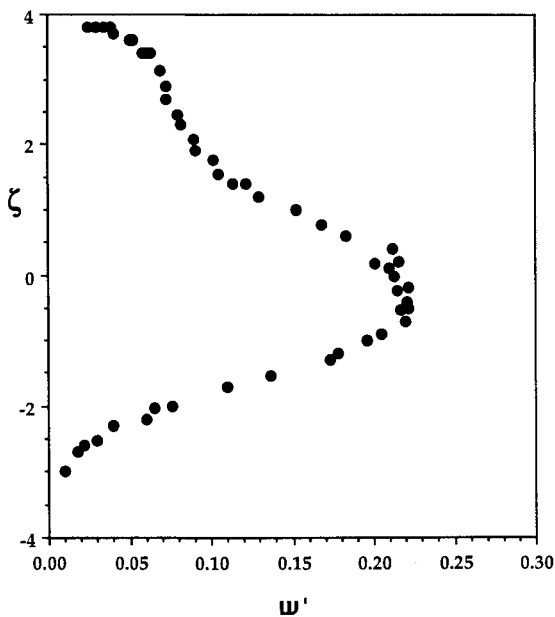


Fig. 12 Vertical profile of the rms fluctuations in the vertical direction at  $\eta = 0$  for  $\zeta_0 = 3.85$ .

with increasing  $|\eta|$  for a given  $\zeta$ , and with increasing  $\zeta$  for  $\eta = 0$ . Figure 12, a vertical profile of  $w'$  at  $\eta = 0$ , shows that  $w'$  decreases almost symmetrically, as in the previous cases, at least for  $|\zeta| < 2$ . However, unlike  $u'$  and  $v'$ ,  $w'$  decreases sharply very near the free surface (within a distance of about one core radius). This signals an interesting metamorphosis as far as the effect of free surface on turbulence is concerned. The turbulence becomes much more anisotropic and the reduction in  $w'$  (the reflection of vertical momentum from the free surface) leads to an increase in  $u'$  and  $v'$ . It is, therefore, important to explore the variation of the turbulent kinetic energy, particularly in the region where the two-dimensionalization of turbulence occurs.

Figure 13 shows the turbulent kinetic energy  $\epsilon_t = (u'^2 + v'^2 + w'^2)/2$  as a function of  $h/h_0 = \zeta/\zeta_0$ . As one might expect,  $\epsilon_t$  is near maximum on the surface normal passing through the vortex center. As the free surface is approached,

$\epsilon_t$  decreases sharply at first to about 0.018 (near  $h/h_0 = 0.6$ ), then remains nearly constant up to about  $h/h_0 = 0.9$ , and then shows (see inset) a slight increase as  $h/h_0 \rightarrow 1$  (the free surface). In other words, the two-dimensionalization of turbulence very near the free surface is not at the expense of total turbulent kinetic energy, and the increase of both  $u'$  and  $v'$  is indeed due to the reflection of vertical momentum from the free surface. In this reflection, the free surface behaves as a scarred surface, exhibiting hydrodynamic roughness as it is seen from below. Had it behaved like a rigid, shear-free boundary, the reflection process would have been relatively simple to interpret. However, the formation of a scar, on the downflow side of the vortex; the unsteady fluctuations associated with the formation, amalgamation, and motion of the whirls (small vortices with axes in the surface-normal direction<sup>7</sup>); and, possibly, the interaction of these scar structures with the fluid (air) directly above render the reflection process much more complex than that in a fully developed turbulent channel flow<sup>13-15</sup> and require a closer examination of the quasi-coherent turbulent structures near the free surface.

The foregoing raises a number of additional questions that must be addressed if one is to understand the two-dimensionalization process and its role in the formation of SAR images: Does  $\epsilon_t$  indeed increase very near the free surface, are there other flow situations (not involving a trailing vortex) that exhibit similar characteristics near the free surface, and how do these structures decay with time or downstream distance. Undoubtedly, these questions are rather complicated, and their numerical resolution will pose severe tests for all turbulence models.

The transition from fully three-dimensional toward two-dimensional turbulence, the slowing down of the decay of kinetic energy, and the strong increase of the length scale have attracted attention in other turbulent flows for a number of years. Jacquin et al.<sup>8</sup> and the numerous references cited therein dealt with the effect of rotation on the two-dimensionalization of turbulence and the strong departure of the length scales from those for an isotropic state.<sup>11</sup> Hunt and Graham<sup>9</sup> investigated theoretically the case of homogeneous freestream turbulence impinging on a rigid wall and found a growing viscous boundary layer adjacent to the free surface and a larger inviscid "source layer." At the edge of the viscous surface layer the kinetic energy of turbulence is the same as in the bulk of the fluid, but the fluid velocity component normal to the surface vanishes, and the energy in this motion is

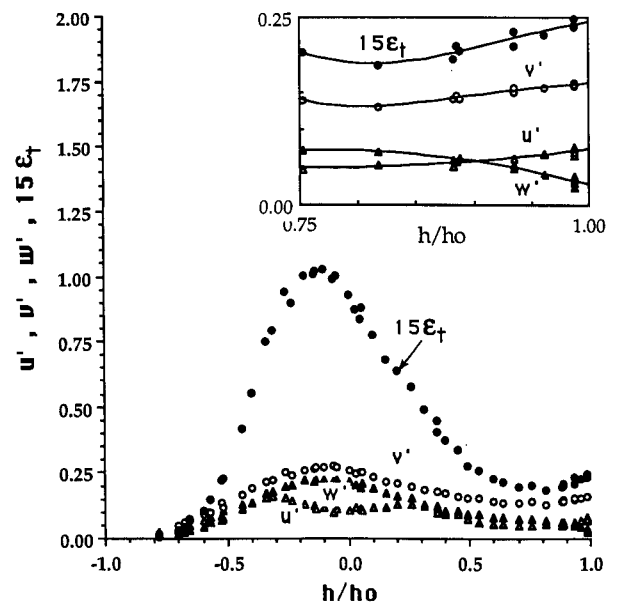


Fig. 13 Vertical profiles of all three rms fluctuations and 15 times the kinetic energy vs  $h/h_0$  for  $\eta = 0$  and  $\zeta_0 = 3.85$ . Inset shows the near-surface values.

partitioned (equally, for an isotropic flow) to the streamwise and lateral motions.

Loewen et al.<sup>10</sup> investigated the statistics of free-surface flow structures generated by a vertical bar grid moving through water in a towing tank. They have found a profusion of coherent surface structures that either rotate (surface eddies), translate (river flow), or are relatively stagnant and that the surface flow is predominantly two dimensional. Their results show that the eddy size distribution gradually shifts to a larger size as turbulence decays, and an increasing fraction of the fluctuating kinetic energy is transferred into "rivers." Brumley<sup>11</sup> and Dickey et al.<sup>12</sup> made turbulence measurements near the free surface in grid-stirred tanks and demonstrated that the true dissipation rate is relatively uniform near the surface, rather than decaying as the fourth power of the distance from the horizontal grid, as it does in the case of deeply submerged grids. Sarpkaya and Suthon<sup>7</sup> suggested, on the basis of their observations, that the free-surface turbulence exhibits features that obey the decay laws of two-dimensional turbulence. Subsequently, Sarpkaya<sup>4,5</sup> has simulated the evolution of near-surface structures by a decaying two-dimensional turbulence through vortex dynamics and has shown that the energy and enstrophy inertial ranges coexist, with an upscale energy transfer (reverse energy cascade) and a downscale enstrophy transfer in the same wave number interval while conserving energy and enstrophy.

Komori et al.<sup>13</sup> made measurements of temperature, velocity, and turbulence fields very close to the free surface in an open-channel flow and found that the vertical motions are damped, whereas the streamwise and spanwise motions are promoted. Subsequently, Rashidi and Banerjee<sup>14</sup> and Lam and Banerjee<sup>15</sup> found, through flow visualizations of bubble streaks near the free surface of an open-channel flow and also through numerical simulations, that the kinetic energy of turbulence is redistributed from the surface-normal to the parallel fluctuations. Their results are quite similar to those obtained by Komori et al.<sup>13</sup> in the range where they may be compared. Lam and Banerjee<sup>15</sup> noted that, unlike the numerical prediction, the experimental values of  $w'$  did not vanish at the interface. They have suggested that "this was probably due to the slight waves present in the experiments." As noted earlier, these experiments are for relatively simple channel flows, containing no trailing vortices or jets.

More recently, Anthony<sup>16</sup> and Anthony and Willmarth<sup>17</sup> made turbulence measurements in a round jet beneath a free surface and found that near the surface  $u'$  and  $v'$  increase, whereas  $w'$  decreases. Their  $\epsilon_t$  data,<sup>17</sup> calculated from their Fig. 4b, are shown in Fig. 14 together with those calculated from the rms data of Lam and Banerjee,<sup>15</sup> Komori et al.,<sup>13</sup> and the present investigation. In doing so, the vertical distance (from the channel bottom, the jet axis, or the vortex axis) was expressed in terms of the relative distance  $h/h_0$ . The turbulent kinetic energy for each case was scaled by its corresponding minimum value. This normalization does not imply identical scaling laws but allows one to compare the decay of  $\epsilon_t$  for the four sets of data considered herein.

The conclusion common to all of the foregoing studies is that the free surface redistributes part or all of the normal turbulent kinetic energy  $w'^2/2$  into the streamwise and spanwise components  $u'^2/2$  and  $v'^2/2$ . The turbulent kinetic energy increases very near the free surface in all of the four sets of data (see inset). The results for the channel and vortex flows (Lam and Banerjee,<sup>15</sup> Komori et al.,<sup>13,18</sup> and the present data) show for  $h/h_0 > 0$  that the values of  $\epsilon_t$  decrease by comparable rates and then acquire nearly constant values in a very thin layer near the free surface. This lends credence to Sarpkaya's<sup>4,5</sup> and Sarpkaya and Suthon's<sup>7</sup> numerical simulation of the evolution of near-surface structures by a decaying two-dimensional turbulence via vortex dynamics (see, e.g., Sarpkaya<sup>21</sup>). The case of the round jet parallel to the free surface is an exception where the turbulent kinetic energy remains nearly constant throughout the region above the jet axis. Apparently, the dynamics of turbulence very close to the free surface (as  $h/h_0 \rightarrow 1$ ) are very complex and significantly different from that near a smooth or rough rigid surface. The role of the near-surface layer, the persistence of  $u'$  and  $v'$  as  $h/h_0 \rightarrow 1$ , the interaction between quasi-two-dimensional coherent structures near the free surface, and the restructuring and modulation of this interaction by wind and contaminants need extensive measurements.

## Conclusions

The interaction of a single turbulent trailing vortex with a deformable free surface has been undertaken for the purpose of exploring the velocity and turbulence field in the vicinity of a clean free surface. The evidence presented herein shows that there are two regions where in one, near the vortex, the turbulent kinetic energy decays rapidly with increasing vertical distance and in the other, very near the free surface (on the order of millimeters), the said energy remains essentially constant. The energy of the vertical velocity fluctuations is redistributed among the lateral and streamwise motions. Even though all four flows discussed herein exhibit, to varying degrees of intensity, the behaviors noted earlier, trailing vortices and open-channel flows delineate the two distinct regions of turbulent energy distribution more emphatically than submerged jets. Finally, it is noted that the results of the present investigation lend further credence to the numerical simulation of the free-surface structures via two-dimensional vortex dynamics.

The use of a turbulent vortex near the free surface of an otherwise smooth uniform flow proved to be a "kernel" experiment toward the elucidation of the dynamical processes in vorticity/free-surface interaction. Detailed measurements of mean velocity and all components of the Reynolds stress tensor are needed toward the development of a predictive model of the vorticity/free-surface interaction. These measurements and the understanding of the character of the quasi-coherent structures near the free surface constitute the essence of the ongoing investigation.

## Acknowledgments

The support of this project by the Office of Naval Research (ONR) is gratefully acknowledged. The authors wish to express their sincere appreciation to Edwin P. Rood (ONR) for his continued encouragement and support.

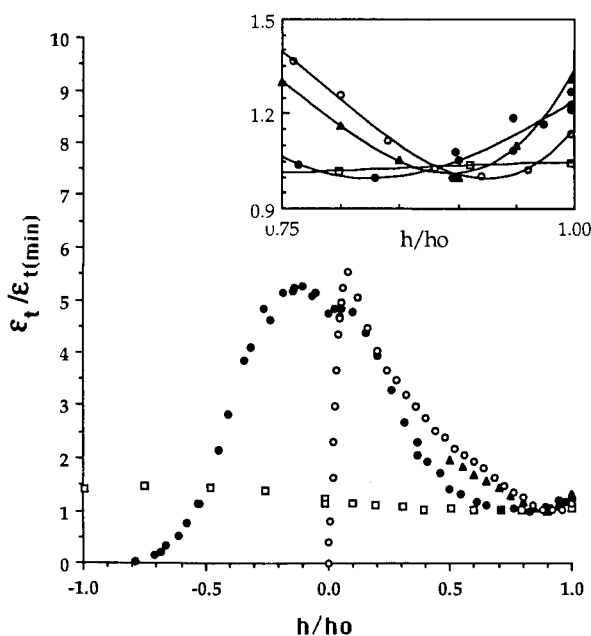


Fig. 14  $\epsilon_t/\epsilon_{t(\min)}$  vs  $h/h_0$  for four flow conditions: •, submerged vortex (present study); ○, open channel (Lam and Banerjee<sup>15</sup>); ▲, open channel (Komori et al.<sup>13</sup>); □, submerged jet (Anthony and Willmarth<sup>17</sup>). Inset shows the near-free-surface values.

## References

- <sup>1</sup>Harvey, J. K., and Perry, F. J., "Flow Field Produced by Trailing Vortices in the Vicinity of the Ground," *AIAA Journal*, Vol. 9, No. 12, 1971, pp. 1659, 1660.
- <sup>2</sup>Shabaka, I. M. M., Mehta, R. D., and Bradshaw, P., "Longitudinal Vortices Imbedded in Turbulent Boundary Layers, Part 1: Single Vortex," *Journal of Fluid Mechanics*, Vol. 155, June 1985, pp. 37-57.
- <sup>3</sup>Sarpkaya, T., "Trailing-Vortex Wakes on the Free Surface," *Proceedings of the 16th Symposium on Naval Hydrodynamics*, National Academy Press, Washington, DC, 1986, pp. 38-50.
- <sup>4</sup>Sarpkaya, T., "Three-Dimensional Interactions of Vortices with a Free Surface," AIAA Paper 92-0059, Jan. 1992.
- <sup>5</sup>Sarpkaya, T., "Interaction of a Turbulent Vortex with a Free Surface," *Proceedings of the Nineteenth Symposium on Naval Hydrodynamics*, National Academy Press, Washington, DC, 1992 (in press).
- <sup>6</sup>Sarpkaya, T., Elnitsky, J., and Leeker, R. E., "Wake of a Vortex Pair on the Free Surface," *Proceedings of the 17th Symposium on Naval Hydrodynamics*, National Academy Press, Washington, DC, 1988, pp. 47-54.
- <sup>7</sup>Sarpkaya, T., and Suthon, P. B. R., "Interaction of a Vortex Couple with a Free Surface," *Experiments in Fluids*, Vol. 11, July 1991, pp. 205-217.
- <sup>8</sup>Jacquín, L., Leuchter, O., and Geffroy, P., "Experimental Study of Homogeneous Turbulence in the Presence of Rotation," *Turbulent Shear Flows 6*, edited by J. C. André, J. Cousteix, F. Durst, B. E. Launder, F. W. Schmidt, and J. H. Whitelaw, Springer-Verlag, Berlin, 1989, pp. 46-57.
- <sup>9</sup>Hunt, J. C. R., and Graham, J. M. R., "Free-Stream Turbulence Near Plane Boundaries," *Journal of Fluid Mechanics*, Vol. 84, Jan. 1978, pp. 209-235.
- <sup>10</sup>Loewen, S., Ahlborn, B., and Filuk, A. B., "Statistics of Surface Flow Structures on Decaying Grid Turbulence," *Physics of Fluids*, Vol. 29, No. 8, 1986, pp. 2388-2397.
- <sup>11</sup>Brumley, B., "Turbulence Measurements near the Free Surface in Stirred Grid Experiments," *Gas Transfer at Water Surfaces*, edited by W. Brutsaert and H. Jirka, Reidel-Dordrecht, The Netherlands, 1984, pp. 83-86.
- <sup>12</sup>Dickey, T. D., Hartman, B., Hammond, D., and Hurst, E., "A Laboratory Technique for Investigating the Relationship Between Gas Transfer and Fluid Turbulence," *Gas Transfer at Water Surfaces*, edited by W. Brutsaert and H. Jirka, Reidel-Dordrecht, The Netherlands, 1984, pp. 93-100.
- <sup>13</sup>Komori, S., Ueda, H., Ogino, F., and Mizushima, T., "Turbulence Structure and Transport Mechanism at the Free Surface in an Open Channel Flow," *International Journal of Heat and Mass Transfer*, Vol. 25, No. 4, 1982, pp. 513-521.
- <sup>14</sup>Rashidi, M., and Banerjee, S., "Turbulence Structure in Free Surface Channel Flows," *Physics of Fluids*, Vol. 31, No. 9, 1988, pp. 2491-2503.
- <sup>15</sup>Lam, K., and Banerjee, S., "On the Condition of Streak Formation in a Bounded Turbulent Flow," *Physics of Fluids A*, Vol. 4, No. 2, 1992, pp. 306-320.
- <sup>16</sup>Anthony, D. G., "The Influence of a Free Surface on the Development of Turbulence in a Submerged Jet with a Clean or Contaminated Free Surface," Ph.D. Thesis, Univ. of Michigan, Dept. of Naval Architecture, Ann Arbor, MI, 1990.
- <sup>17</sup>Anthony, D. G., and Willmarth, W. W., "Turbulence Measurements in a Round Jet beneath a Free Surface," *Journal of Fluid Mechanics*, Vol. 243, Oct. 1992, pp. 699-720.
- <sup>18</sup>Komori, S., Nagaosa, R., Murakami, Y., Chiba, S., Ishii, K., and Kuwahara, K., "Direct Numerical Simulation of Three-Dimensional Open-Channel Flow with Zero-Shear Gas-Liquid Interface," *Physics of Fluids A*, Vol. 5, No. 1, 1993, pp. 115-125.
- <sup>19</sup>Durand, W. F. (ed.), *Aerodynamic Theory*, Vol. III, Dover, New York, 1963, pp. 280-306.
- <sup>20</sup>Rosenhead, L., "The Spread of Vorticity in the Wake Behind a Cylinder," *Proceedings of the Royal Society of London, Series A: Mathematical and Physical Sciences*, Vol. 127, No. 2, 1930, pp. 590-612.
- <sup>21</sup>Sarpkaya, T., "Computational Methods with Vortices—1988 Freeman Scholar Lecture," *Journal of Fluids Engineering, Transactions of ASME*, Vol. 111, No. 1, 1989, pp. 5-52.